Optical response of reconstructed GaP(001) surfaces

M. Zorn*
Institut für Festkörperphysik, Technische Universität Berlin, Sekr. PN 6-1, Hardenbergstraße 36, D-10623 Berlin, Germany

B. Junno
Department of Solid State Physics, Lund University, Box 118, S-221 00 Lund, Sweden

T. Trepk
Institut für Festkörperphysik, Technische Universität Berlin, Sekr. PN 6-1, Hardenbergstraße 36, D-10623 Berlin, Germany

S. Bose
Institut für Theoretische Physik, Technische Universität Berlin, Sekr. PN 7-1, Hardenbergstraße 36, D-10623 Berlin, Germany

L. Samuelson
Department of Solid State Physics, Lund University, Box 118, S-221 00 Lund, Sweden

J.-T. Zettler and W. Richter
Institut für Festkörperphysik, Technische Universität Berlin, Sekr. PN 6-1, Hardenbergstraße 36, D-10623 Berlin, Germany
(Received 25 January 1999)

GaP(001) surfaces were found to reconstruct with (2×1) or (2×4) symmetry under surface conditions corresponding to a high or low V/III surface stoichiometry ratio, respectively. These surface reconstructions, identified by reflection high-energy electron diffraction, have been prepared in a chemical beam epitaxy (CBE) system by varying the sample temperature. Reflectance anisotropy spectra (RAS) of these surfaces have been taken under both CBE and metal-organic vapor phase epitaxy conditions. Three different phases of (2×4) symmetry have been distinguished according to their characteristic RAS response in agreement with recent theoretical predictions [A.M. Frisch, W.G. Schmidt, J. Bernholc, M. Pristovsek, N. Esser, and W. Richter, Phys. Rev B **60**, 2488 (1999)]. For the (2×1) reconstruction a line-shape analysis of the RAS signatures was performed and their temperature shifts have been compared to the respective shifts of the bulk critical points. These experiments indicate the GaP(001)-(2×1) surface dielectric anisotropy originating from transitions between bulk states modified by the surface due to band-folding effects and anisotropic shifts of the E_1 and E_0' critical point energies. [S0163-1829(99)12439-1]

I. INTRODUCTION

GaP represents together with InP the binary boundary system for $In_xGa_{1-x}P$ that presently is one of the most promising materials both for high-performance laser structures in the visible to near-infrared (vis-NIR) spectroscopic region and high-frequency hetero-bipolar-transistors (HBT) devices for the wireless communication electronics.[1] GaP itself is also of technological importance, e.g., for the fabrication of light-emitting diodes (LED's) because its fundamental band gap is in the visible region of the light spectrum.

In this work we focus on the optical properties of reconstructed GaP(001) surfaces by applying reflectance anisotropy spectroscopy which is sometimes also called reflectance difference spectroscopy (RAS/RDS).[2,3] Our aim is twofold: Firstly, a detailed study of the changing reflectance anisotropy signatures under variation of the V-III surface stoichiometry and temperature will complement recent theoretical treatment of the GaP(001)-(2×4) (Ref. 4) and will ease respective future work on the GaP(001)-(2×1) reconstruction. Secondly, once the RAS response of GaP(001), InP(001), and $In_xGa_{1-x}P(001)$ surfaces is reasonably well understood, the surface status of this technologically important class of III-V materials can be determined *in situ*. This will allow for the control of the surface stoichiometry during the formation of heterointerfaces for reaching optimum electronic interface properties.

The surface response of GaAs(001) (Refs. 5–7 and InP(001) (Refs. 8–11) has been studied by a number of groups and a correlation between the detailed structure of their main reconstructions and their respective surface optical properties has been established. For GaP(001), however, only preliminary RAS studies[12,13] are available. The GaP bulk optical properties have been measured by spectroscopic ellipsometry at room temperature[14,15] and in the temperature range from 15 K up to 640 K.[16]

In the experiments reported here, it is found that when exposed to similar surface conditions GaP(001) and InP(001) surfaces form similar surface reconstructions. We will, therefore, compare our GaP(001) results to recent InP(001) studies.[8,9]

Under high P supply the InP(001) surface forms a number of reconstructions when the temperature T is increased: $c(4\times4)$,(2×2), (2×1), (2×4)-P^+, and (2×4)-P^- with decreasing P contents on the surface due to the enhanced P desorption at higher temperatures.[8] [The greek letters nor-

mally used to indicate different reconstructions of the same $(n\times m)$ symmetry are often differently defined in experimental [reflection high-energy electron diffraction (RHEED) and low-energy electron diffraction (LEED)] and theoretical publications. Therefore, different InP(001) and GaP(001) surface phases of the same symmetry are denoted here by the phosphorus supply conditions they belong to (P^+ and P^- for the high and low P supply, respectively)]. As the InP(001)-(2×4)-P^+ does not exist under reduced P supply, a direct transition from (2×2) to (2×4)-P^- reconstruction occurs. The existence of two different (2×4) phases and the remarkably similar RAS spectra of the InP-(2×4)-P^+ and the GaAs-$\beta2(2\times4)$ reconstructions[8,17] are in excellent agreement with recent theoretical work where two stable InP(001)-(2×4) surface phases have been determined by *ab initio* surface total-energy calculations.[18]

In former UHV studies of GaP(001) the following surface reconstructions have been reported: (4×2),[19–23] (2×4),[12,20,24,25] and (1×2).[19] The (4×2) was found to show up after ion bombardment and annealing (IBA) which is known to result in group-III-rich surfaces. The (2×4) and the (1×2) characteristically are found under conditions where a sufficiently high phosphorus background can be supposed due to former growth of P-containing materials. Very recent investigations suggest that the reported (4×2) and (1×2) reconstructions in fact are (2×4) and (2×1) reconstructions when correctly defining the crystal axes.[4]

The surface optical response of (2×4) reconstructed GaP(001) surfaces has only very recently been treated theoretically based on density-functional theory in local-density approximation (DFT-LDA).[4] These calculations predicted three stable (2×4) surface reconstructions: $\beta2(2\times4)$, mixed-dimer (2×4), and top-Ga-dimer (2×4),[4] but only two of them could be verified experimentally.[4] This could be, however, due to the limitations of the preparation technique used in Ref. 4 where reconstructions have been investigated resulting from carefully performed thermal desorption of phosphorus from a GaP(001) surface initially capped by amorphous phosphorus (a-P). Because of the high-temperature necessary for desorption of a-P (about 690 K) and due to the kinetics of the desorption process it is supposed that only a limited number of reconstructions could be prepared. Therefore, we performed experiments in chemical beam epitaxy (CBE) and metal-organic vapor phase epitaxy (MOVPE) growth systems in order to complete the theoretical studies of the GaP(001)-(2×4) surface dielectric anisotropy in Ref. 4. These experiments allowed us to freely adjust the GaP surface chemical potential between being highly P-rich and highly Ga-rich by supplying P and Ga at various temperatures to just-grown, atomically-smooth surfaces. We also measured the temperature-dependent GaP bulk dielectric function and therefore could compare the line-shape and temperature shift of the GaP(001) surface dielectric anisotropy (SDA) signatures to those of the GaP bulk critical points and those of equally reconstructed GaAs and InP surfaces.

This paper is organized as follows: First, in Sec. III A, the temperature-dependent GaP bulk dielectric function is determined and a line-shape analysis in the parabolic band approximation[26] for measuring the temperature-dependent bulk critical points is performed. Thereafter, in Sec. III B, the GaP(001) reconstructions prepared in a CBE system are identified by their RHEED patterns and assigned to their respective RAS spectra. In Sec. III C we focus on the (2×1) reconstruction that is formed under conditions of a very high V/III surface stoichiometry ratio. Finally, in Sec. III D, three different phases of the GaP(001)-(2×4) reconstruction are identified and their RAS spectra are compared to theoretical predictions.

II. EXPERIMENT

Clean and absorbate-free GaP(001) surfaces have been prepared both under UHV conditions in a CBE growth system and under gas-phase conditions in a MOVPE facility.

In CBE triethylgallium (TEGa) and tertiarybuthylphosphine (TBP) were used for the GaP epitaxy. After oxide desorption, a buffer layer was grown to prepare a smooth surface. The chamber pressure, dominated by the group-V pressure, was varied from 10^{-5} to 10^{-4} mbar. Different surface reconstructions were established by varying the sample temperature. A RHEED system allowed for the measurement of the surface reconstruction under varying P supply while taking RAS spectra simultaneously trough a strain-reduced quartz port.[27] This enabled a direct assignment of the RAS spectra to certain surface reconstructions. The temperature was measured using a pyrometer and verified by the temperature dependence of significant features in the RAS spectra.

The MOVPE system used here is a horizontal reactor equipped with both a RAS spectrometer and a spectroscopic ellipsometer.[28] After oxide desorption under phosphine (PH_3) GaP layers were grown using trimethylgallium (TMGa) and phosphine as precursors. The surface stoichiometry of the GaP surfaces was changed by varying the phosphine pressure between 0 and 100 Pa and exposing the surface to a TMGa pulse.

The substrates used in the CBE system were both-side polished. This has an influence on the RAS spectra below the fundamental gap where the sample is transparent and the back-side reflectance contributes its own, not necessarily well-defined, anisotropy.

In both CBE and MOVPE the reflectance anisotropy was measured as the difference in reflectance between the two GaP(001) crystalline main axes along $[\bar{1}10]$ and [110],

$$\frac{\Delta r}{\bar{r}}=2\frac{r_{[\bar{1}10]}-r_{[110]}}{r_{[\bar{1}10]}+r_{[110]}} \tag{1}$$

using a setup according to Aspnes.[29]

Signatures in the measured RAS $\mathrm{Re}(\Delta r/r)$ spectra are similar to those of the absorption anisotropy $\mathrm{Im}(\Delta\varepsilon_s)$ of the surface region only in spectral regions of low bulk absorption, where ε_b is real. Therefore, the surface dielectric anisotropy (SDA) $\Delta\varepsilon_s d$ is usually calculated from the RAS spectra[30]

$$\Delta\varepsilon_s d=\frac{\lambda(\varepsilon_b-1)}{4\pi i}\frac{\Delta r}{r}, \tag{2}$$

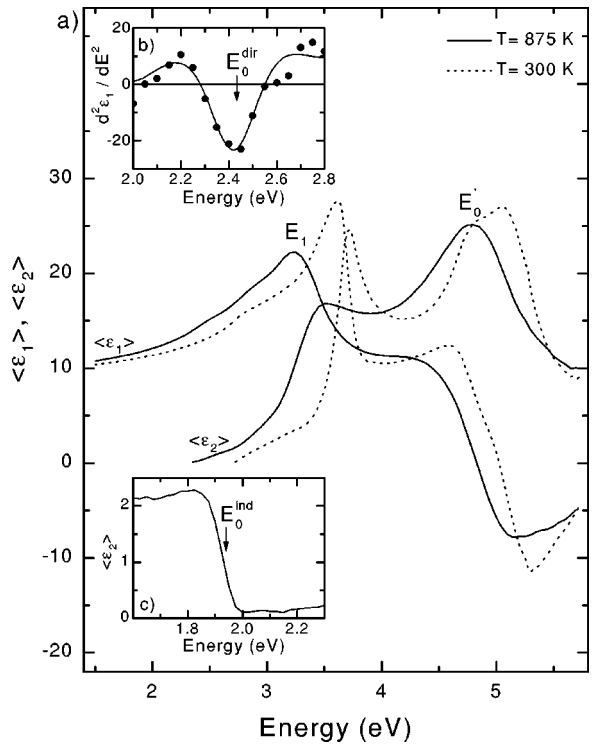

FIG. 1. (a) Real and imaginary part, $\langle \varepsilon_1 \rangle$ and $\langle \varepsilon_2 \rangle$, respectively, of the GaP bulk dielectric function at 300 and 875 K. Inset (b) shows the second derivative of $\langle \varepsilon_1 \rangle$ at 875 K [measurement (points) and fit (solid line)] as used for the determination of E_0^{dir}. Inset (c) gives the depolarization-induced signature in $\langle \varepsilon_2 \rangle$ at E_0^{ind}.

where $\varepsilon_b \cong \langle \varepsilon_b \rangle$ is the measured bulk dielectric function, d is the effective thickness of the anisotropic surface layer ($d \ll \lambda$), and λ is the wavelength of the light.

The ellipsometer additionally used in MOVPE is of the so-called rotating polarizer, sample, analyzer type.[31] Ellipsometry measures the complex ratio ρ of the reflectance parallel (p) and perpendicular (s) to the plane of incidence,

$$\rho = \frac{r_p}{r_s}. \tag{3}$$

Assuming the epitaxially grown surface to be ideally smooth, the GaP bulk dielectric function ε_b was derived from ρ according to

$$\langle \varepsilon_b \rangle = \sin^2\Phi_0 \left[1 + \tan^2\Phi_0 \left(\frac{1-\rho_2}{1+\rho} \right) \right] \tag{4}$$

with Φ being the angle of incidence. The surface, however, has optical properties different from the bulk. Fortunately, this modifies the measured bulk dielectric function only slightly and is indicated as usual by replacing ε_b by the effective dielectric function $\langle \varepsilon_b \rangle$ with $\varepsilon_b \cong \langle \varepsilon_b \rangle$.

III. RESULTS AND DISCUSSION

A. Bulk dielectric function

The experimentally determined GaP bulk dielectric function is given in Fig. 1(a) as measured at 300 and 875 K. Features in the spectra correlated to critical points in the band structure[32] can clearly be observed. The fundamental optical gap E_0^{ind} [2.26 eV at room temperature (RT) (Ref. 33 and Fig. 4)] of GaP is indirect which is therefore only weakly absorbing at photon energies between E_0^{ind} and its direct optical gap E_0^{dir} [2.74 eV at RT (Fig. 4)]. Ellipsometry, when using rotating polarizers, is not sensitive to weakly absorbing materials and therefore precise data for the imaginary part $\langle \varepsilon_2 \rangle$ of the GaP bulk dielectric function around and below E_0^{dir} cannot be easily taken. The energetic position, however, of E_0^{dir} can be determined by line-shape analysis within the parabolic band approximation of the real part $\langle \varepsilon_1 \rangle$ of the GaP bulk dielectric function.[16] Figure 1, inset (b), gives the second derivative of $\langle \varepsilon_1 \rangle$ that was used for determining the energy position of the GaP lowest direct gap E_0^{dir}. For determining the temperature dependence of the indirect gap E_0^{ind} (respective older data given in Refs. 34–36 turned out to not be precise enough) we took advantage of an experimental detail: GaP wafers polished at both sides cause depolarization effects in the ellipsometry measurement in spectral regions where GaP is transparent (i.e., below the lowest optical gap). The small but clearly resolved depolarization induced signature in the imaginary part of the bulk dielectric function $\langle \varepsilon_2 \rangle$ was used for measuring the temperature-dependent shift of the indirect gap E_0^{ind} [Fig. 1(c)]. The measured thermal shift of the E_0^{ind}, E_0^{dir}, and E_1 critical points is given in Fig. 4.

B. GaP(001) reconstructions according to RHEED and their characteristic RAS spectra

In the CBE studies reported here, surface reconstructions of (2×1) and (2×4) symmetry were identified by RHEED, depending on the V/III surface stoichiometry ratio which changes with temperature and P and/or Ga supply to the surface. The RAS spectra in Fig. 2(a) have been taken simultaneously along with the RHEED measurements. They change characteristically in shape with increasing temperature, indicating the transition from the initial (2×1) towards the final (2×4) reconstruction. At least one intermediate phase of (2×4) symmetry seems to exist having a different RAS response than the high-temperature (2×4) phase. A direct transition from the low-temperature (2×1) [spectrum (i) in Fig. 2] towards the high-temperature (2×4) [spectrum (v)] would give simply a downshift of the low-energy RAS minimum at 2.2 eV. In the experiment, however, the minimum at 2.2 eV disappears at 880 K [spectrum (iii)]. The respective RAS spectrum is supposed to correspond to a different phase of the GaP(001)-(2×4) reconstruction. For InP(001) and GaAs(001) based on total-energy calculations it was suggested in Ref. 18 that a $\beta2(2\times4)$ phase is stable under high group-V supply. For proving if this applies also for GaP(001) we compared the RAS spectra of these three materials by introducing a procedure which normalizes the spectra to their respective bulk critical points. The normalized 880 K GaP RAS spectrum is plotted along in Fig. 2(b) with the respective InP(001)-(2×4)-P^+ spectrum from Ref. 8 and the $\beta2(2\times4)$ spectrum of GaAs(001) from Ref. 17. After this normalization the imaginary parts of the bulk dielectric function of GaP, InP, and GaAs have also essentially the same line shape [Fig. 2(c)].

The normalized RAS spectra in Fig. 2(b) of all the three materials turn out to be very similar by displaying a maxi-

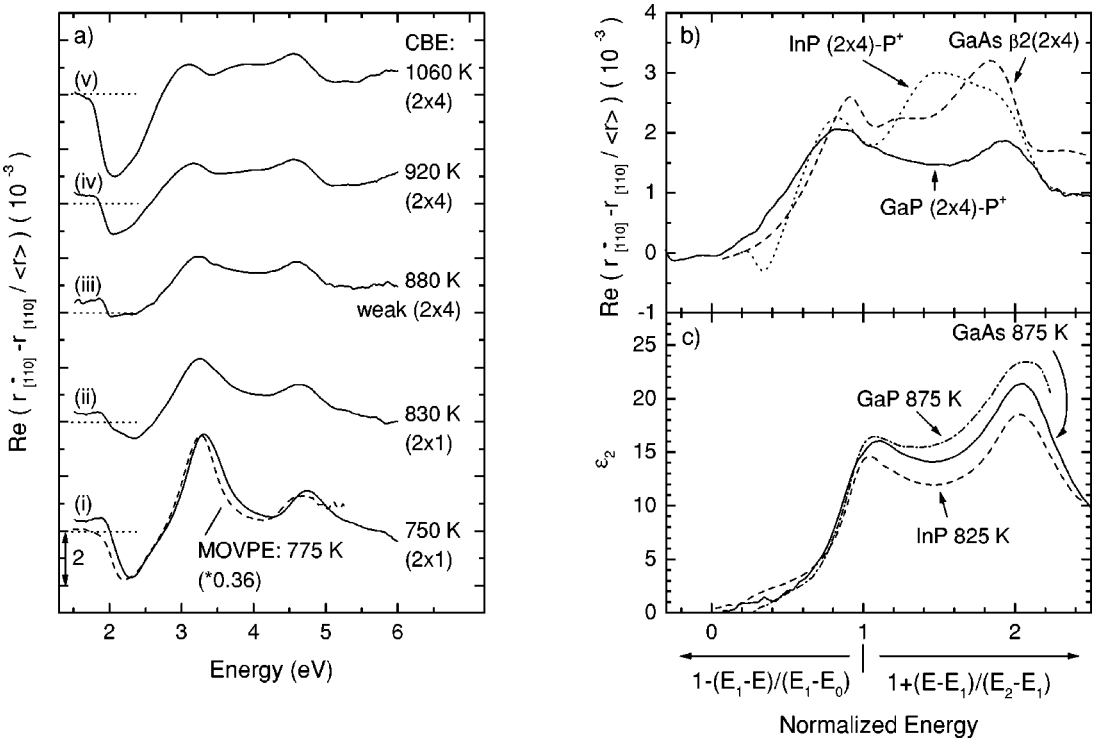

FIG. 2. (a) RAS spectra taken in the CBE system for different temperatures under constant phosphorus supply. The surface reconstructions were determined by simultaneously performed RHEED measurements. For comparison a RAS spectrum taken in MOVPE under phosphorus stabilization is added (dashed line, scaled by factor 0.36). Spectrum (iii), corresponding to a phosphorus-rich (2×4) reconstruction [(2×4)-P^+], is compared in (b) to the respective spectrum of InP(001) and the $\beta2(2\times4)$ spectrum of GaAs(001) by normalizing the photon energy to the bulk critical points. The InP spectrum in (b) is taken from Ref. 8 and the GaAs spectrum from Ref. 17. (c) shows the normalized imaginary part of the respective bulk dielectric functions. The formulas used for the normalization are shown in the figure.

mum slightly below the E_1 critical point, a second maximum at E_2, and a very small anisotropy below E_1. We regard this similarity in the normalized optical response as a strong indication that these reconstructions for all the three materials are based on very similar atomic configurations. This is in agreement with total-energy calculations predicting a $\beta2(2\times4)$ reconstruction being stable under high group-V supply for GaP(001),[4] InP(001),[18] and GaAs(001) (Ref. 37) surfaces.

At temperatures higher than 900 K [spectra (iv) and (v)] the minimum at 2 eV again clearly forms. Both spectra differ in the depth of the minimum at 2 eV and an additional small peak around 4 eV that is characteristic for spectrum (v). In Sec. III D we will verify by desorption/adsorption studies that spectra (iv) and (v) in Fig. 2(a) in fact represent two further, well distinguished phases of the GaP(001)-(2×4) reconstruction.

C. GaP(001) surfaces under very high P supply: the (2×1) reconstruction

At very high P supply the same (2×1) RAS response is measured under gas-phase and UHV conditions [see Fig. 2(a), spectra (i)]. We therefore studied its line-shape and temperature dependence in a MOVPE system, where simultaneous RAS and spectroscopic ellipsometry (SE) measurements can be performed. Figure 3 gives the temperature-dependent surface dielectric anisotropy (SDA) of the (2×1) reconstructed GaP(001) surface as calculated according to Eq. (2). These $\Delta\varepsilon_2 d$ spectra represent the absorption anisotropy due to surface effects only. In contrast to the directly measured $\Delta r/r$ spectra in Fig. 2(a) [spectrum (i)], the influence of the bulk dielectric function is now eliminated in the high-energy part of the spectra also.

The 300 K SDA spectra of the (2×1) reconstructed GaP(001) is compared in Fig. 3 to the first derivative of the imaginary part (dash-dotted line) of the respective bulk dielectric function, yielding a good agreement for $E \geqslant 3.5$ eV. For the low-energy part of these spectra a sharp negative onset of the RAS exactly at the indirect bulk gap E_0^{ind} is characteristic.

To study this similarity of surface and bulk optical signatures in more detail we compared in Fig. 4 the temperature dependence of two characteristic features, $A_{(2\times1)}$ and $B_{(2\times1)}$, of the SDA spectra to the temperature dependence of the bulk critical points E_0^{ind}, E_0^{dir}, and E_1. $A_{(2\times1)}$ marks the onset of the anisotropy in the low-energy range (2.2 eV at RT), and $B_{(2\times1)}$ corresponds to the higher-energetic derivativelike RAS signature (3.7 eV at RT). The onset of the surface anisotropy in the low-energy region of the (2×1)-like spectra $A_{(2\times1)}$ is obviously directly correlated to the fundamental band gap E_0^{ind}. This could be explained by band-folding effects due to which close to the surface formerly bulk-forbidden transitions become allowed causing an anisotropic optical response.[38] The $B_{(2\times1)}$ signature closely follows the bulk E_1 transition in its spectral position and temperature dependence. Because of its first-derivative-like line shape we suggest a surface-induced anisotropic shift of the E_1 position to be responsible for the $B_{(2\times1)}$ signature.

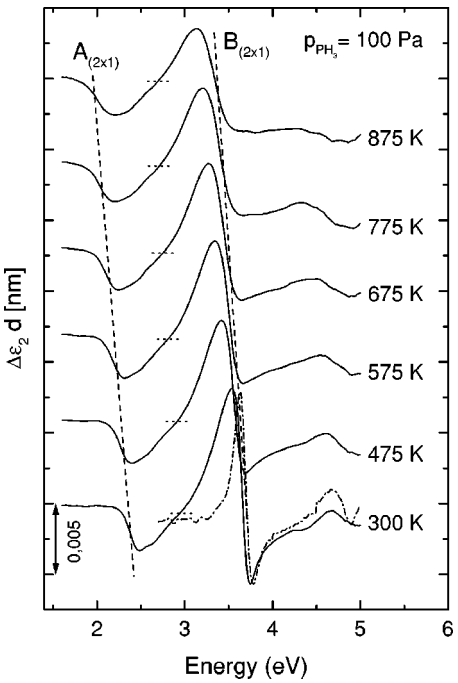

FIG. 3. Surface dielectric anisotropy (SDA) of GaP(001)-(2 $\times$1) under very high phosphorus supply between 300 and 875 K (MOVPE, phosphorus pressure 100 Pa). The energy positions of the two characteristic signatures $A_{(2\times1)}$ and $B_{(2\times1)}$ were determined from the zeros of the second derivative SDA spectra. The temperature shifts of $A_{(2\times1)}$ and $B_{(2\times1)}$ are indicated by dashed lines. For comparison the first derivative of the imaginary part of the bulk dielectric function $d\varepsilon_2/dE$ is also shown (300 K, dash-dotted line, scaled by factor 8.3×10^{-5}).

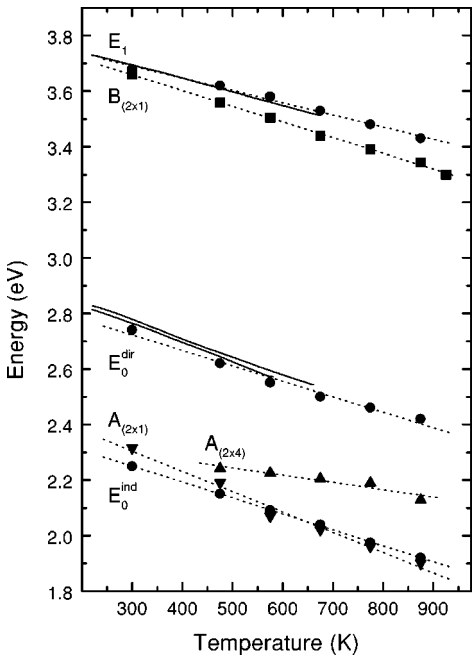

FIG. 4. Temperature dependence of the bulk critical points (E_0^{ind}, E_0^{dir}, and E_1) and of characteristic features in the SDA spectra ($A_{(2\times1)}$, $B_{(2\times1)}$, and $A_{(2\times4)}$ according to Figs. 3 and 5). Data from the literature for E_0^{dir} (Refs. 16 and 34) and E_1 (Ref. 16) are added for comparison (solid lines).

Summarizing the experimental results under very high phosphorus supply we conclude that the GaP(001)-(2$\times$1) surface reconstruction corresponds to a highly phosphorus-rich surface. Even under the most phosphorus-rich conditions (low temperature and high phosphorus pressure) no transition to another group-V-rich surface reconstruction [like the $c(4\times4)$ on GaAs (Ref. 5) or InP (Refs. 8 and 9)] was observable. The SDA spectra of this surface seem to be dominated by contributions of surface-modified bulk states. Phosphorus dimers along the $[\bar{1}10]$ direction are likely to terminate this surface as has been proposed by Kobayashi *et al.*[39] There, however, differently to our findings, the P dimers were directly correlated to the $B_{(2\times1)}$ signature. Future scanning tunneling microscopy (STM) investigations will have to clarify if the (2$\times$1) RHEED and LEED patterns measured at this surface are caused by a homogeneous reconstruction or if, as in the case of InP,[40] a superposition of different reconstruction domains leads to the diffraction pattern.

D. The GaP(001)-(2×4) surface phases: Time-resolved studies during P desorption and Ga pulsing

RAS spectra characteristic for the GaP(001)-(2$\times$4) reconstruction show up under gas-phase (MOVPE) conditions when the phosphine stabilization is switched off. Figure 5(a) gives RAS spectra taken at high time resolution during the P desorption process. The initial spectrum, still under phosphine stabilization, clearly corresponds to a (2$\times$1) reconstruction [Fig. 2(a), spectrum (i)]. A spectrum assigned to $\beta2(2\times4)$ in Sec. III B [Fig. 2(a), spectrum (iii)] appears after 90 sec and is classified here as (2×4)-P^+ because it belongs obviously to the most P-rich (2×4) phase. The RAS signal continues to change slowly for approximately 400 sec until it stabilizes in a shape that corresponds to the 920 K spectrum in CBE [Fig. 2(a), spectrum (iv)]. This spectrum, classified here as (2×4)-P^-, remains unchanged for tens of minutes stabilized only by the weak background P pressure from the reactor. When, however, a short Ga pulse is added to this surface (by switching on TMGa for approximately 4 sec, corresponding to about 1 ML of GaP), another spectrum, $(2\times4)-$Ga, appears similar to the 1060 K spectrum in CBE [Fig. 2(a), spectrum (v)]. It characteristically has a deeper minimum around 2 eV and an additional small maximum at 3.7 eV as compared to the (2×4)-P^- spectrum. This (2×4)-Ga spectrum cannot be changed furthermore by additional Ga pulses and therefore is expected to correspond to the most Ga-rich stable surface phase.

The three GaP(001)-(2$\times$4) reconstruction phases (2 $\times$4)-P^+, (2×4)-P^-, and (2×4)-Ga obviously form with decreasing V/III surface stoichiometry ratio both in CBE [Fig. 2(a), spectra (iii), (iv), (v)] and MOVPE [Fig. 5(a)].

The RAS minimum around 2.0 eV [$A_{(2\times4)}$ in Fig. 5(a)] is characteristic both for the (2×4)-P^- and (2×4)-Ga spectra. Its energy position is clearly below E_0^{dir} and the complete signature extends even below the E_0^{ind} gap. It must be caused, therefore, by an additional surface absorption along the [110] direction and must involve true surface states. Moreover, the $A_{(2\times4)}$ peak clearly has a temperature depen-

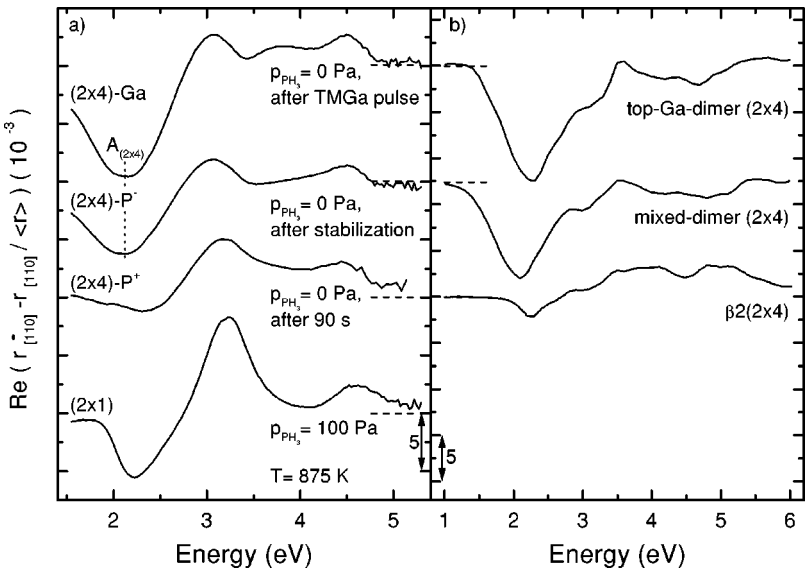

FIG. 5. (a) RAS spectra taken in MOVPE at 875 K for different surface conditions: (i) under a phosphorus supply of 100 Pa, (ii) 90 sec after the phosphine was switched off, (iii) 15 min after the phosphine was switched off, and (iv) after exposing the surface to a short TMGa pulse. (b) Calculated spectra from total-energy calculations (DFT-LDA) using the indicated surface reconstructions (taken from Ref. 4). The temperature dependence of the energy position of the dominating minimum around 2.2 eV of the spectra (iii) and (iv) is plotted in Fig. 4 ($A_{(2\times4)}$).

dence less than the bulk transitions, indicating a reduced temperature shift of the surface states involved in this transition (Fig. 4).

We now compare these experimental results to the calculations recently published in Ref. 4 where three (2×4) phases have been predicted from total-energy calculations. We assume that the surface phases (2×4)-P^+, (2×4)-P^-, and (2×4)-Ga, experimentally found with decreasing V/III surface stoichiometry ratio, correspond to a $\beta2(2\times4)$, mixed-dimer (2×4), and top-Ga-dimer (2×4) reconstruction change. This assumption is also supported by the good agreement, after a rigid shift in energy due to the DFT-LDA gap problem,[41] between the measured spectra and those calculated in Ref. 4 [Fig. 5(b)].

Both, the DFT-LDA calculations [Ref. 4 and Fig. 5(b)] and our own preliminary tight-binding calculations (computational details are given in Ref. 38 and surface atomic positions have been used as *ab initio* calculated in Ref. 4) characterize the $A_{(2\times4)}$ peak being clearly dominated by a surface-to-surface transition. The tight-binding calculations further suggest that the respective transition is basically one from binding Ga dimer states to unoccupied Ga orbitals at the outer Ga atoms of the mixed-dimer (2×4) and the top-Ga-dimer (2×4) surface structure. Obviously, the dimers in the upper atomic layer (Ga-As mixed dimer or Ga-Ga top dimer, respectively) are not directly involved in the transition. This would explain the similarity between the RAS spectra of the (2×4)-P^- (mixed-dimer) and the (2×4)-Ga (top-Ga-dimer) surface reconstruction. Similar contributions of Ga dimers have been found also for RAS signatures of $\alpha(2\times4)$ reconstructed GaAs(001) surfaces[37] and during CBE growth of GaAs.[42]

We speculate that the higher ability of the surface atomic configuration to compensate the temperature-induced lattice expansion (via bending and tilting) is responsible for the reduced temperature shift of the $A_{(2\times4)}$ RAS signature. This hand-waving explanation is consistent with the chemical modulation spectroscopy investigations by Postigo *et al.*[43] where the effect of strain to the GaP(001) surface optical properties was studied. It should, of course, be verified by future calculations that should artificially expand the bulk lattice constant below and check the surface response.

IV. CONCLUSIONS

The surface optical properties of reconstructed GaP(001) surfaces were studied under UHV and gas-phase conditions and compared to recent theoretical results. Two surface reconstructions, (2×1) and (2×4), have been identified by simultaneously performed RAS and RHEED measurements. The (2×1) reconstruction appears under high phosphorus pressure and lower temperatures. Its surface anisotropy is closely correlated to bulk critical points featuring an abrupt onset at the E_0^{ind} gap and a derivativelike signature in the high-energy part of the RAS spectra. When the P supply to the surface is reduced, three different (2×4) phases are formed distinguished by their characteristic RAS signatures. This experimental result is consistent with recent theoretical work predicting three stable GaP(001)-(2×4) phases: $\beta2(2\times4)$, mixed-dimer (2×4), and top-Ga-dimer (2×4), respectively. All the main features of the measured RAS signatures characteristic for the three (2×4) phases are closely resembled in the recently published theoretically calculated optical response.[4]

ACKNOWLEDGMENTS

The authors gratefully acknowledge the support by the BMBF (01 BT 310/835), the DAAD and the Deutsche Forschungsgemeinschaft (SFB 296).

*FAX: +49-30-31421769. Electronic address: zorn@physik.tu-berlin.de

[1] S.S. Lu, IEEE Electron Device Lett. **13**, 214 (1992).
[2] M. Zorn, J. Jönsson, W. Richter, J.-T. Zettler, and K. Ploska, Phys. Status Solidi A **152**, 23 (1995).
[3] D.E. Aspnes, Mater. Sci. Eng., B **30**, 109 (1995).
[4] A.M. Frisch, W.G. Schmidt, J. Bernholc, M. Pristovsek, N. Esser, and W. Richter, Phys. Rev. B **60**, 2488 (1999).
[5] I. Kamiya, D.E. Aspnes, H. Tanaka, L.T. Florez, J.P. Harbison, and R.H. Bhat, Phys. Rev. Lett. **68**, 627 (1992).

[6] I. Kamiya, D.E. Aspnes, L.T. Florez, and J.P. Harbison, Phys. Rev. B **46**, 15 894 (1992).
[7] J. Rumberg, J.-T. Zettler, K. Stahrenberg, K. Ploska, W. Richter, L. Däweritz, P. Schützendübe, and M. Wassermeier, Surf. Sci. **337**, 103 (1995).
[8] K.B. Ozanyan, P.J. Parbrook, M. Hopkinson, C.R. Whitehouse, Z. Sobiesierski, and D.I. Westwood, J. Appl. Phys. **82**, 474 (1997).
[9] M. Zorn, T. Trepk, J.-T. Zettler, B. Junno, C. Meyne, K. Knorr, T. Wethkamp, M. Klein, M. Miller, W. Richter, and L. Samuelson, Appl. Phys. A: Mater. Sci. Process. **65**, 333 (1997).
[10] T.K. Johal, S.D. Barrett, M. Hopkinson, P. Weightman, and J.R. Power, J. Appl. Phys. **83**, 480 (1998).
[11] P.J. Parbrook, K.B. Ozanyan, M. Hopkinson, C.R. Whitehouse, Z. Sobiesierski, and D.I. Westwood, Appl. Phys. Lett. **73**, 345 (1998).
[12] K. Knorr, M. Pristovsek, U. Resch-Esser, N. Esser, M. Zorn, and W. Richter, J. Cryst. Growth **170**, 230 (1997).
[13] J.S. Luo, J.F. Geisz, J.M. Olson, and M.-C. Wu, J. Cryst. Growth **174**, 558 (1997).
[14] D.E. Aspnes and A.A. Studna, Phys. Rev. B **27**, 985 (1983).
[15] H. Yoshikawa and S. Adachi, Jpn. J. Appl. Phys., Part 1 **35**, 5946 (1996).
[16] S. Zollner, M. Garriga, J. Kircher, J. Humliček, M. Cardona, and G. Neuhold, Phys. Rev. B **48**, 7915 (1993).
[17] J.-T. Zettler, J. Rumberg, K. Ploska, K. Stahrenberg, M. Pristovsek, W. Richter, M. Wassermeier, P. Schützendübe, J. Behrend, and L. Däweritz, Phys. Status Solidi A **152**, 35 (1995).
[18] W.G. Schmidt, F. Bechstedt, N. Esser, M. Pristovsek, Ch. Schulz, and W. Richter, Phys. Rev. B **57**, 14 596 (1998).
[19] A.J. van Bommel and J.E. Crombeen, Surf. Sci. **76**, 499 (1978).
[20] J.N. Baillargeon, K.Y. Cheng, and K.C. Hsieh, Appl. Phys. Lett. **56**, 2201 (1990).
[21] N. Sanada, M. Shimomura, Y. Fukada, and T. Sato, Appl. Phys. Lett. **67**, 1432 (1995).
[22] M.M. Sung and J.W. Rabalais, Surf. Sci. **365**, 136 (1996).
[23] M. Naitoh, A. Watanabe, A. Konishi, and S. Nishigaki, Jpn. J. Appl. Phys., Part 1 **35**, 4789 (1996).
[24] M. Yoshikawa, A. Nakamura, T. Nomura, and K. Ishikawa, Jpn. J. Appl. Phys., Part 1 **35**, 1205 (1996).
[25] P.A. Postigo, T. Utzmeier, G. Armelles, and F. Briones, J. Cryst. Growth **175/176**, 298 (1997).
[26] D.E. Aspnes, Surf. Sci. **37**, 418 (1973).
[27] A.A. Studna, D.E. Aspnes, L.T. Florez, B.J. Wilkens, J.P. Harbison, and R.E. Ryan, J. Vac. Sci. Technol. A **7**, 3291 (1989).
[28] J.-T. Zettler, T. Wethkamp, M. Zorn, M. Pristovsek, C. Meyne, K. Ploska, and W. Richter, Appl. Phys. Lett. **67**, 3783 (1995).
[29] D.E. Aspnes, R. Bhat, E. Colas, L.T. Florez, J.P. Harbison, M.K. Kelly, V.G. Keramidas, M.A. Koza, and A.A. Studna, Proc. SPIE **1037**, 2 (1988).
[30] D.E. Aspnes, J. Opt. Soc. Am. **63**, 1380 (1973).
[31] R.M.A. Azzam and N.M. Bashara, *Ellipsometry and Polarized Light* (Elsevier Science, Amsterdam, 1977).
[32] J.R. Chelikowsky and M.L. Cohen, Phys. Rev. B **14**, 556 (1976).
[33] P.J. Dean and D.G. Thomas, Phys. Rev. **150**, 690 (1966).
[34] V.K. Subashiev, and G.A. Chalikyan, Phys. Status Solidi **13**, K91 (1966).
[35] M.R. Lorenz, G.D. Pettit, and R.C. Taylor, Phys. Rev. **171**, 876 (1968).
[36] M.B. Panish and H.C. Casey, Jr., J. Appl. Phys. **40**, 163 (1969).
[37] A.I. Shkrebtii, N. Esser, W. Richter, W.G. Schmidt, F. Bechstedt, B.O. Fimland, A. Kley, and R. Del Sole, Phys. Rev. Lett. **81**, 721 (1998).
[38] R. Del Sole, in *Photonic Probes of Surfaces*, edited by P. Halevi (Elsevier Science, Amsterdam, 1995), Chap. 4, p. 133.
[39] N. Kobayashi, Y. Kobayashi, and K. Uwai, J. Cryst. Growth **170**, 225 (1997).
[40] P. Vogt, A.M. Frisch, T. Hannappel, S. Visbeck, F. Willig, Ch. Jung, N. Esser, W. Braun, and W. Richter, Phys. Status Solid B **215**, 737 (1999).
[41] F. Bechstedt, in *Festkörperprobleme/Advances in Solid State Physics* , edited by U. Roessler (Vieweg, Braunschweig, 1992), Vol. 32, p. 161.
[42] T. Farrell, D. Hill, T.B. Joyce, T.J. Bullough, and P. Weightman, J. Cryst. Growth **175/176**, 1217 (1997).
[43] P.A. Postigo, G. Armelles, and F. Briones, Phys. Rev. B **58**, 9659 (1998).